Scene Visibility Complexity in Flatland

Jaume Rigau, Miquel Feixas, Mateu Sbert

Institut d'Informàtica i Aplicacions, Universitat de Girona
rigau|feixas|mateu@ima.udg.es

Abstract

The objective of this paper is to study scene visibility complexity in flatland, expressed by scene visibility mutual information. To achieve this aim we consider several 2D scenes to try to understand the relationship of the complexity with the number, size, and relative position of the objects within the scene, the form of the enclosure and the number of patches. Particularly, we analyze the growth of complexity when the scene is close to a singularity that can occur in relation to the position of the objects or the form of the enclosure. Finally we present a simple and preliminary scene classification.

Keywords: complexity, information theory, Monte Carlo, radiosity, visibility

1. Introduction

Complexity is an active research area, and recently many complexity measures have been proposed from different fields. But, what is complexity? Complexity is related to difficulty: "The meaning of this quantity should be very close to certain measures of difficulty concerning the object or the system in question: the difficulty of constructing an object, the difficulty of describing a system, the difficulty of reaching a goal, the difficulty of performing a task, and so on" [14]. From another point of view, complexity is related to understanding: "The concept of complexity is closely related to understanding, in so far as the latter is based upon the accuracy of model descriptions of the system obtained using a condensed information about it. Hence, a theory of complexity could be viewed as a theory of modelling" [1]. In the particular case of a 3D scene, the complexity measure that we have proposed in our previous work [7, 8] is scene mutual information, which can be interpreted as the difficulty of computing accurately the visibility and radiosity in a scene. Scene mutual information, which is an information theory measure, quantifies the information transfer in a scene, and also the correlation or dependence among all their points or patches. In [7, 8], we established a close relationship between complexity and discretization.

Now we apply mutual information for studying the scene visibility complexity in flatland. One of the main objetives in studying flatland is to explore some new aspects about complexity and discretization which can later be extended to 3D scenes. On the one hand, there are problems which will be easier to study in 2D, but on the other, 2D studies present their own particular problems, as in robot motion. Some of the most important applications of scene complexity are in the cost prediction for visibility computations and in the development of meshing strategies to obtain an optimal discretization. The study of 2D scene visibility complexity has potential applications in fields such as animation, robot motion and architectural design.

In this paper we measure the complexity of several 2D scenes and we analyze in a simple and extensive way the behaviour of scene visibility complexity in relation to quantity, size, and position of the objects, and also to the enclosure form.

The organisation of this paper is as follows: In section 2 we present the framework for studying scene visibility complexity in flatland. In section 3 we define the scene visibility complexity in flatland and discuss the results presented. In section 4 we compute the complexity of different scenes, we analyze the main reasons for the growth in complexity, and we propose a preliminary scene classification.

2. Framework

2.1. Radiosity and form factors in flatland

The *2D radiosity equation* for the illumination in a diffuse environment can be written in the form

$$B(x) = E(x) + R(x) \int_{\mathcal{L}} B(x') V(x,x') \frac{\cos\theta \cos\theta'}{2r} dL' \quad (1)$$

where $B(x)$ is the radiosity in the point x, $E(x)$ is the emittance, $R(x)$ is the reflectance, $\mathcal{L}$ is the set of segments that form the environment, x, x' are points on segments of the environment, dL' is a length differential at point x', r is the distance between x and x', $V(x,x')$ is the visibility flag between x and x', θ, θ' are the angles which the normals at x, x' form with the line joining them, and $V(x,x')\frac{\cos\theta\cos\theta'}{2r}$ is the differential form factor between x and x'.

To solve the radiosity equation we can use a finite element approach and discretise the environment into n_p patches, considering the radiosities, emissivities and reflectances constant over the patches. In this way we transform the integral equation into the radiosity system of equations [12]

$$B_i = E_i + R_i \sum_{j=1}^{n_p} F_{ij} B_j \quad (2)$$

where the *form factors* F_{ij} between the segments i and j are only dependent on the geometry of the scene

$$F_{ij} = \frac{1}{L_i} \int_i \int_j \frac{\cos\theta_i \cos\theta_j}{2r} V_{ij} dL_i dL_j \quad (3)$$

and fulfil the following properties

$$L_i F_{ij} = L_j F_{ji} \quad \forall i, j \quad (4)$$

$$\sum_{j=1}^{n_p} F_{ij} = 1 \quad \forall i \quad (5)$$

The form factor F_{ij} describes what fraction of the energy emitted by patch i will hit another patch j. Also, the form factor F_{ij} can be considered as the probability of a line that exiting from or crossing i lands on j. If we identify the lines connecting two patches with visibility, the form factor will give us the *visibility* between patches [18, 19].

2.2. Markov chains for scene visibility in flatland

A *random walk* [17] in a scene can be considered as a *Markov chain* [15]. This is a discrete stochastic process defined over a set of n states S which can be described by a *transition probability matrix* P. This matrix has one row and one column for each state in S. The element $P_{j|i}$ in the matrix P is the probability that the next visited state for an imaginary particle will be j, given that the current state is i. Thus, for all $i, j \in S$, we have $\sum_{j=1}^{n} P_{j|i} = 1$. Under certain conditions, which are fulfilled in the context of this paper, the probabilities of finding the particle in each state i converge to a *stationary distribution* $w = (w_1, \ldots, w_n)$ after a number of steps. The stationary or equilibrium probabilities w_i fulfil the relation $w_i = \sum_{j=1}^{n} w_j P_{i|j}$. For the Markov Chains we deal with in this paper, the stationary distribution satisfies the reciprocity relation $w_i P_{j|i} = w_j P_{i|j}$.

In [7] we studied *discrete 3D scene visibility complexity* by letting the states $i = 1, \ldots, n_p$ correspond to the patches of a scene (n_p denotes the number of patches) and the transition probabilities P_{ij} with the form factors F_{ij}. It can be shown [7] that in flatland the stationary probabilities of the resulting Markov Chain are given by $w_i = L_i / L_T$, the relative length of the patch i (L_i is the length of patch i and L_T is the total length of all segments of the scene). This Markov chain will be used in the study of *discrete scene visibility complexity* in flatland.

When the states form a countable set, as above, the Markov Chain is called a *discrete* chain. When the states are not countable, the chain is called *continuous*. For instance, when taking infinitesimal lengths dx at each point x on the set of segments $\mathcal{L}$ of the scene as states and differential form factors $F(x,y)$ with $x, y \in \mathcal{L}$ as transition probabilities, a continuous Markov Chain with stationary distribution $w(x) = 1/L_T$ results. This Markov Chain will be used in the study of *continuous scene visibility complexity* in flatland.

2.3. Information theory

In this section, we present some basic concepts of information theory [2, 4]. The *Shannon entropy* H of a *discrete* random variable X with values in the set $\{a_1, a_2, \ldots, a_n\}$ is defined as

$$H(X) = -\sum_{i=1}^{n} p_i \log p_i \quad (6)$$

where $p_i = Pr[X = a_i]$, the logarithms are taken in base 2, and also we take $0 \log 0 = 0$. As $-\log p_i$ represents the *information* associated with the result a_i, the entropy gives the average information or the *uncertainty* of a random variable. The unit of information is called *bit*.

If we consider another random variable Y with probabilities q_i corresponding to values in the set $\{b_1, b_2, \ldots, b_m\}$, the *joint entropy* of X and Y is defined as

$$H(X,Y) = -\sum_{i=1}^{n} \sum_{j=1}^{m} p_{ij} \log p_{ij} \quad (7)$$

where $p_{ij} = Pr[X = a_i, Y = b_j]$, and the *conditional entropy* is defined as

$$H(X|Y) = -\sum_{j=1}^{m} \sum_{i=1}^{n} p_{ij} \log p_{i|j} \quad (8)$$

where $p_{i|j} = Pr[X = a_i | Y = b_j]$. The Bayes theorem expresses the relation between the different probabilities: $p_{ij} = q_j p_{i|j} = p_i p_{j|i}$. If X and Y are *independents*, we have $p_{ij} = p_i q_j$. The conditional entropy can be thought of in terms of a *channel* whose input is the random variable X and whose

output is the random variable Y. $H(X|Y)$ corresponds to the uncertainty in the channel input from the receiver's point of view.

The *mutual information* between two random variables X and Y is defined as

$$I(X,Y) = H(X) - H(X|Y) = \sum_{i=1}^{n}\sum_{j=1}^{m} p_{ij} \log \frac{p_{ij}}{p_i q_j} \qquad (9)$$

From the above definitions, we can obtain the following properties: $I(X,Y) \geq 0$ and $I(Y,X) = I(X,Y)$. The mutual information represents the amount of information that one random variable, the output of the channel, gives about a second random variable, the input of the channel. $I(X,Y)$ is a measure of the shared information between X and Y.

The joint entropy of n random variables is defined as

$$H(X_1,\ldots,X_n) = H(X_1) + H(X_2|X_1) + \ldots + H(X_n|X_1,\ldots,X_{n-1}) \qquad (10)$$

and the *entropy rate* or *entropy density* of a chain of random variables is defined by

$$\begin{aligned} h &= \lim_{n\to\infty} \frac{1}{n} H(X_1,X_2,\ldots,X_n) \\ &= \lim_{n\to\infty} H(X_n|X_{n-1},\ldots,X_1) \end{aligned} \qquad (11)$$

representing the average information content per output symbol. It is the uncertainty associated with a given symbol if all the preceding symbols are known and can be viewed as the intrinsic *unpredictability* or the irreducible *randomness* associated with the chain [11].

In particular, a Markov chain can be considered as a chain of random variables complying with

$$H(X_n|X_1,X_2,\ldots,X_{n-1}) = H(X_n|X_{n-1}) \qquad (12)$$

An important result is the following theorem: A Markov chain with equilibrium distribution has entropy rate or information content

$$\begin{aligned} h &= \lim_{n\to\infty} \frac{1}{n} H(X_1,X_2,\ldots,X_n) \\ &= -\sum_{i=1}^{n} w_i \sum_{j=1}^{n} P_{j|i} \log P_{j|i} \end{aligned} \qquad (13)$$

where w_i is the equilibrium distribution. Note that h coincides with $H(X|Y)$, the conditional entropy of a channel, where the distribution probability of X, Y is $\{w_i\}$ and $p_{j|i} = P_{j|i}$.

In the *continuous* case, mutual information between two continuous random variables is the limit of their discretised versions [4]. Thus, discrete mutual information I converges to continuous mutual information I^c when the number n of "patches" tends to infinity: $I^c = \lim_{n\to\infty} I$. On the other hand, entropy of a continuous random variable does not equal the entropy of the discretised random variable in the limit of finer discretization. Especifically, discrete entropy tends to infinity when the "patch" sizes tend to zero and continuous entropy changes when the random variable is scaled [4].

2.4. Scene visibility complexity and optimal discretization

Over the last twenty years, many different ways to quantify complexity have been presented from different fields (automata, information theory, computer science, physics, biology, neuroscience, ...). In our previous work, an information theory measure, mutual information, which quantifies the degree of *structure* or *correlation* of a system has been applied to scene visibility. On the one hand, continuous scene visibility mutual information has been proposed as an absolute measure of the complexity of scene visibility, while on the other, discrete mutual information was proposed as the complexity measure of discretised scene visibility. Also, we have shown that when a patch is refined into m subpatches discrete mutual information increases or remains the same and therefore continuous mutual information of a scene is the least upper bound to discrete mutual information: $I \leq I^c$.

In [7], we established two proposals which show a close relationship between complexity and discretization: (i) the greater the complexity the more difficult it is to get a discretization which expresses with precision the visibility or radiosity of a scene and (ii) among different discretizations of a scene the best is the one with the highest discrete mutual information. Thus, while continuous mutual information expresses how difficult it is to discretise a scene to compute accurately the visibility, discrete mutual information gives us a measure of how well we have done it.

With reference to the relationship between complexity and entropy, the latter, which measures unpredictability or randomness, does not capture structure [9,10] but, quoting Shalizi and Crutchfield, "*complexity (in our sense) and randomness each capture a useful property necessary to describe how a process manipulates information*" [5]. In our case, mutual information and entropy are clearly complementary, and while mutual information measures the accuracy of the discretization, entropy is closely related to form factor computational cost with the Monte Carlo method [7].

3. Scene visibility complexity in flatland

The most basic information theory definitions applied to 3D scene visibility were presented in [7]. In this section, Shannon entropy, entropy rate, and discrete and continuous mutual information are adapted to flatland by only changing the area of each patch with the length of each patch. Flatland visibility and radiosity is studied in [13,16]. Next, using different computational methods (string rule and Monte Carlo simulation for form factor computation, exact solution of the continuous mutual information integral), we calculate the complexity of diverse scenes.

3.1. Discrete entropy and discrete mutual information

3.1.1. Definitions

As we have seen (section 2.2), a random walk in a discretised 2D scene can be considered as a Markov chain where $P_{j|i} = F_{ij}$, $n = n_p$, and $w_i = \frac{L_i}{L_T}$. In a 2D scene, the Bayes theorem can be expressed by the following property of the form factors

$$p_{ij} = \frac{L_i}{L_T} F_{ij} = \frac{L_j}{L_T} F_{ji} \tag{14}$$

Thus, the *scene visibility entropy rate*, or simply *scene visibility entropy*, is defined by

$$H_s = -\sum_{i=1}^{n_p} \frac{L_i}{L_T} \sum_{j=1}^{n_p} F_{ij} \log F_{ij} \tag{15}$$

and measures the average uncertainty that remains about the patch j visited next (*destination* patch) when an imaginary particle undergoing an infinite random walk, with the form factors as transition probabilities, is known to be on a given patch i (*source* patch).

The Shannon entropy of the stationary distribution, which we call *scene visibility positional entropy*, is defined by

$$H_p = -\sum_{i=1}^{n_p} \frac{L_i}{L_T} \log \frac{L_i}{L_T} \tag{16}$$

and reflects the uncertainty on the position (patch) of a particle travelling an infinite random walk.

The *discrete scene visibility mutual information* is defined by the difference of positional entropy and entropy rate

$$\begin{aligned} I_s &= H_p - H_s \\ &= -\sum_{i=1}^{n_p} \frac{L_i}{L_T} \log \frac{L_i}{L_T} + \sum_{i=1}^{n_p} \frac{L_i}{L_T} \sum_{j=1}^{n_p} F_{ij} \log F_{ij} \end{aligned} \tag{17}$$

and can be interpreted as the average amount of information that the destination patch conveys about the source patch, and vice versa. Consequently, I_s *is a measure of the average information transfer in a scene*. Moreover, it can be expressed as the Kullback-Leibler "distance" [4], or discrimination, between the scene probability distribution $\{p_{ij}\} = \{\frac{L_i}{L_T} F_{ij}\}$ and the independence distribution $\{p_i q_j\} = \{\frac{L_i L_j}{L_T^2}\}$. Thus, the mutual information can be rewritten as

$$I_s = \sum_{i=1}^{n_p} \sum_{j=1}^{n_p} \frac{L_i F_{ij}}{L_T} \log \frac{\frac{L_i F_{ij}}{L_T}}{\frac{L_i L_j}{L_T^2}} = \sum_{i=1}^{n_p} \sum_{j=1}^{n_p} \frac{L_i F_{ij}}{L_T} \log \frac{F_{ij} L_T}{L_j} \tag{18}$$

and interpreted as a "distance" to independence.

The *scene visibility joint entropy* is defined by

$$\begin{aligned} H_j &= -\sum_{i=1}^{n_p} \sum_{j=1}^{n_p} \frac{L_i}{L_T} F_{ij} \log(\frac{L_i}{L_T} F_{ij}) \\ &= 2H_s + I_s = 2H_p - I_s \end{aligned} \tag{19}$$

and can be interpreted as the average uncertainty on which pair of successive patches of the trajectory of a random walk the particle is travelling between.

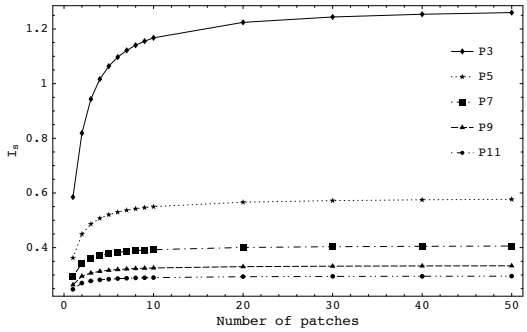

Figure 1: *I_s values (in vertical axis) for regular polygons of 3, 5, 7, 9, and 11 sides with different regular discretizations of their sides. Horizontal axis is labeled by the number of patches for each side.*

3.1.2. Results and discussion

In order to illustrate the above definitions, we will study two sets of scenes: regular polygons and three scenes with 64 squares in each. In the first case, the form factors have been computed exactly by the string rule [16], and in the second, 10^5 global lines have been cast to obtain an approximated Monte Carlo solution for the form factors [18, 20], by counting the number of intersections between pairs of segments which are visible. In this case, the mean square error for all form factors [6] $E(MSE) = \frac{1}{N}(n_p - \sum_i \sum_j F_{ij}^2)$, where N is the total number of intersections, has also been calculated.

For regular polygons, i.e. from 3 to 11 sides, we observe in figure 1 that maximum mutual information (discrete scene visibility complexity) corresponds to an equilateral triangle ($I_s \approx 1.26$) and minimum to a polygon of 11 sides ($I_s \approx 0.3$): there is a higher correlation between the edges of a triangle than between the ones of an 11-sided polygon. Thus, continuing this sequence of regular polygons, it seems that the minimum complexity has to correspond to a circle. In the next section we will analyze its complexity.

Figure 2 shows that the minimum scene visibility entropy corresponds to an equilateral triangle and the maximum to an 11-sided polygon. This fact can also be tested in table 2, even with the same total number of patches. For instance, the entropy H_s of an equilateral triangle with 150 patches ($H_s \approx 5.97$) is less than the entropy H_s of a pentagon with 150 patches ($H_s \approx 6.66$). In fact, continuing the sequence of regular polygons, maximum entropy should correspond to a circle.

Figure 3 shows the behaviour of the entropy and mutual information of an equilateral triangle when the number of patches grows. In accordance with the theory, while entropy

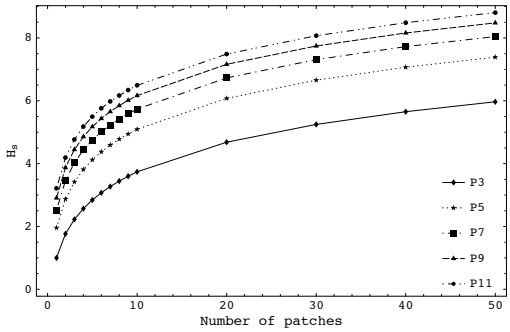

Figure 2: *H_s values (in vertical axis) for regular polygons of 3, 5, 7, 9, and 11 sides with different regular discretizations of their sides. Horizontal axis is labeled by the number of patches for each side.*

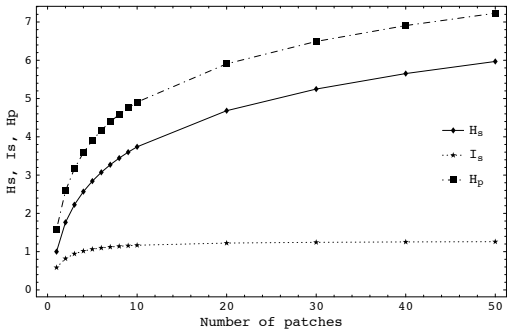

Figure 3: *H_p, H_s and I_s values (in vertical axis) for an equilateral triangle with different regular discretizations of its sides. Horizontal axis is labeled by the number of patches for each side.*

increases clearly with the number of patches, mutual information appears to converge to a determined point.

For the scenes with 64 squares (figure 4/table 1), we observe that maximum complexity, or correlation, is obtained in figure 4a, and maximum entropy in figure 4c. The complexity of a square empty scene ($I_s \approx 0.76$ for 20 patches on each segment) increases outstandingly when we add 64 little squares in its interior (from $I_s \approx 5$ to $I_s \approx 6.15$). With respect to mean square error for all form factors, the greater the entropy the greater the error [7]. When the number of patches tends to infinity, entropy and computational error tend to infinity. So, for a given computational error, we need to cast more lines for a scene with higher entropy. In table 1, H_p should be equal in the three cases, but the difference is due to the computational error.

In general, we can conclude:

- Maximum complexity is obtained in scenes with privileged visibility directions, and maximum entropy in the contrary case.
- While entropy and computational error increase unboundedly with the number of patches, discrete scene complexity seems to converge very slowly to a finite value.
- In line with intuition, complexity grows with the number of objects within the scene.

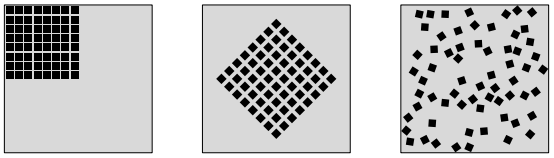

(a) 6.852 (b) 5.792 (c) 5.372

Figure 4: *I_s^c value for three scenes with 64 squares in each. The enclosure is regularly discretised into 80 patches.*

scene	H_s	I_s	H_p	$E(MSE)$
a	2.238	6.150	8.388	0.001766
b	2.986	5.407	8.393	0.002377
c	3.430	5.001	8.431	0.002830

Table 1: *H_p, H_s, I_s and $E(MSE)$ values for the scenes of figure 4.*

3.2. Continuous mutual information

3.2.1. Definition

As we have seen (section 2.2), we can obtain the continuous expression for the above discrete formulae using the following substitutions:

- Each state by an infinitesimal length and each summatory by an integral. For instance, $\sum_{i=1}^{n_p}\sum_{j=1}^{n_p} F_{ij}$ by $\int_{x\in\mathcal{L}}\int_{y\in\mathcal{L}} F(x,y)dxdy$, where $\mathcal{L}$ stands for the segments in the scene.
- $\frac{L_i}{L_T}$ by $\frac{1}{L_T}$. This means substituting the discrete probability of patch i by the continuous probability of selecting any point.
- F_{ij} by $F(x,y)$. This means substituting a patch-to-patch form factor by a point-to-point one. Remember that the value of $F(x,y)$ is $\frac{cos\theta_x cos\theta_y}{2d(x,y)}$ for mutually visible points, zero otherwise, being θ_x and θ_y the angles which the normals at x, y form with the segment joining x and y, and $d(x,y)$ the distance between x and y.

Thus, discrete mutual information converts into continuous mutual information

$$I_s^c = \log L_T + \int_{x\in\mathcal{L}}\int_{y\in\mathcal{L}} \frac{1}{L_T} F(x,y)\log F(x,y)dxdy$$

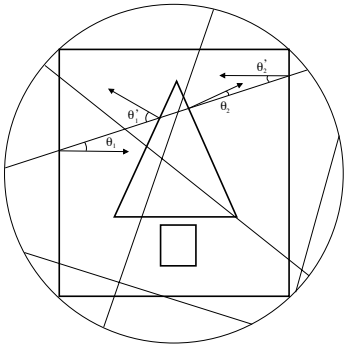

Figure 5: *Global lines are used to compute I_s^c. Lines are generated using a random point on a random diameter.*

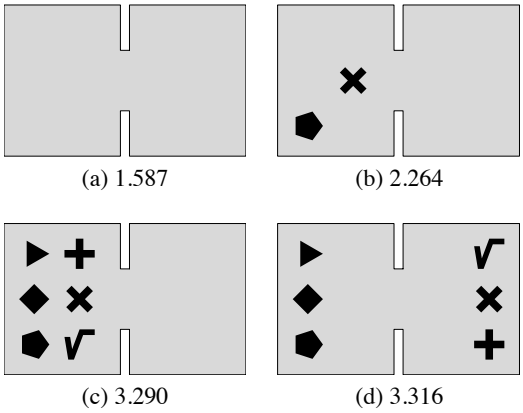

(a) 1.587 (b) 2.264

(c) 3.290 (d) 3.316

Figure 6: *I_s^c value for a room with diverse objects.*

$$= \int_{x\in\mathcal{L}}\int_{y\in\mathcal{L}} \frac{1}{L_T} F(x,y)\log(L_T F(x,y))dxdy \qquad (20)$$

This integral can be solved by Monte Carlo integration. Similarly to [7], the computation can be done efficiently by casting global lines uniformly distributed upon segments [3] (see figure 5). Thus, continuous mutual information can be aproximated by

$$\begin{aligned} I_s^c &\approx \frac{1}{N}\sum_{k=1}^{N}\log(L_T F(x_k,y_k)) \\ &= \frac{1}{N}\sum_{k=1}^{N}\log(\frac{L_T cos\theta_x cos\theta_y}{2d(x,y)}) \end{aligned} \qquad (21)$$

where N is the total number of pairs of points considered, which is the total number of intersections divided by two.

3.2.2. Results and discussion

As we have seen in section 2.4, I_s^c (scene visibility complexity) is the least upper bound to I_s. This fact, which is essential in the study of discretization, is illustrated by the results obtained in this section. Continuous mutual information is computed for three sets of scenes: regular polygons, a square with 64 squares within it, and a room with diverse objects. In all cases, we have solved the Monte Carlo integral by casting global lines, but in the first case we have also calculated the closed form of I_s^c for a circle, an equilateral triangle, a square, and an hexagon.

number of sides	H_s / I_s *10*	*30*	*50*	I_s^c
3	3.739 1.168	5.248 1.244	5.969 1.260	1.284
4	4.590 0.732	6.138 0.769	6.867 0.777	0.788
5	5.094 0.550	6.657 0.572	7.389 0.577	0.583
6	5.455 0.452	7.025 0.467	7.758 0.470	0.475
7	5.737 0.393	7.311 0.404	8.045 0.406	0.408
8	5.969 0.353	7.545 0.362	8.281 0.363	0.366
9	6.166 0.326	7.745 0.332	8.480 0.333	0.336
10	6.338 0.306	7.918 0.311	8.654 0.312	0.314
11	6.491 0.290	8.072 0.295	8.808 0.296	0.297
12	6.628 0.279	8.210 0.282	8.946 0.283	0.284

Table 2: *H_S (top), I_S (bottom) and I_s^c values for regular polygons from 3 to 12 sides with different regular discretizations of their sides (10, 30, and 50 patches for each side).*

For regular polygons, table 2 groups the discrete and continuous results, and we can see that I_s^c is the upper bound of the discrete ones. The complexity of regular polygons is very low. In the other scenes (figures 4 and 6), we observe once again how complexity grows with the introduction of objects in the scene.

As we show in figure 7, continuous mutual information is very cheap to compute because with fewer lines cast than in the discrete case the value obtained is sufficiently accurate.

The closed form solution of the continuous mutual information integral for some regular polygons is shown in table 3.

The complexity of a circle requires special attention. Be-

scene	*exact value*			*MC simulation*
triangle	$\log_2 \frac{18}{e^2}$	$\simeq$	1.285	1.284
square	$\log_2 \frac{8(1+\sqrt{2})}{e^{1+\sqrt{2}}}$	$\simeq$	0.789	0.788
hexagon	$\log_2 \frac{e^{\sqrt{3}-4}324(7+4\sqrt{3})}{168+97\sqrt{3}}$	$\simeq$	0.475	0.475
circle	$\log_2 \frac{\pi}{e}$	$\simeq$	0.209	0.209

Table 3: *Exact I_s^c values for a circle and three regular polygons compared with results obtained by Monte Carlo simulation.*

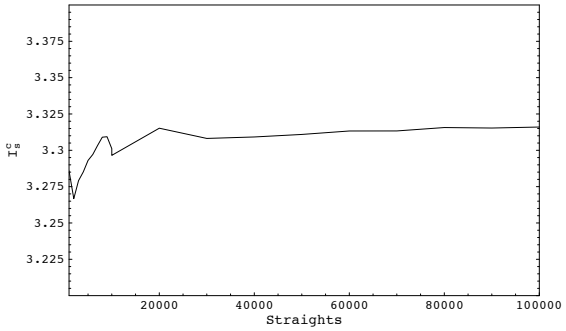

Figure 7: *Behaviour of I_s^c value with the number of lines cast. These results correspond to figure 6(d).*

cause a sphere has zero complexity, we could expect the same for a circle. However, null complexity for the sphere is intimately related to the fact that a uniform line is generated by selecting two random points on its surface. This is no longer true for the circle: selecting random points on its perimeter will not yield a uniform density. Thus, unlike the case of a sphere where, for two spherical patches i and j, $F_{ij} = A_j/A_{sphere}$ (A_j is the area of patch j, A_{sphere} is the total area of the sphere), in the case of a circle, $F_{ij} \neq L_j/L_{circle}$.

Proposition: A scene with zero scene visibility complexity does not exist in flatland.

Proof: Imagine a scene discretised into equal length for all patches. Zero complexity would require all form factors to be equal, including F_{ii} for all i. However, due to symmetry, he latter is only possible in a circle. But, in general, the circle fulfils $F_{ij} \neq F_{ik}$ for $j \neq k$. In conclusion, a scene with zero complexity does not exist in flatland.

We can conclude that:

- In line with theory, I_s^c is the least upper bound to I_s
- I_s^c is easy and cheap to calculate for whatever scene
- A figure with zero complexity does not exist in flatland.

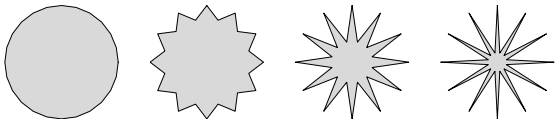

(a) 0.232 (b) 1.966 (c) 5.236 (d) 6.915

Figure 8: *I_s^c value for a 24-sided regular polygon and three 12 pointed star.*

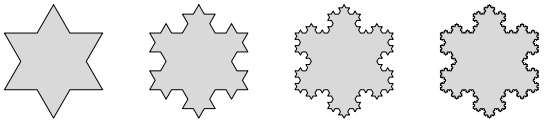

(a) 1.910 (b) 2.950 (c) 4.258 (d) 5.726

Figure 9: *I_s^c value for Von Koch fractals.*

4. Towards a scene classification

In this section we want to present a simple scene classification based on complexity and study the main reasons for the growth in complexity. We compute the complexity of some empty scenes and after that we analyze other scenes with objects placed inside.

4.1. Some study cases

First, we will compute the complexity of four sequences of scenes: the formation of a 12 pointed star, the Von Koch fractal, triangles, and an L-shaped room. After, we will study two particular sequences of scenes: a scene with three objects which increase in size and an expansion of 16 squares from the center of a scene to its walls.

Starting with a polygon of 24 edges, with a complexity very similar to the one of a circle, if we continue closing the edges as shown in figure 8, the complexity increases noticeably due to the growth of the interaction between the edges. In the Von Koch fractal (figure 9), a similar thing happens: by increasing the number of corners, the correlation increases.

In the case of figures 10 and 11, we show how complexity increases when the scene becomes less regular. Going from an equilateral triangle to the triangle in figure 10(d), complexity increases. The same thing happens when we convert a square to a rectangle.

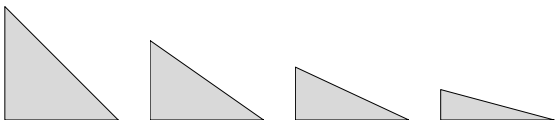

(a) 1.493 (b) 1.530 (c) 1.787 (d) 2.311

Figure 10: *I_s^c value for different triangles.*

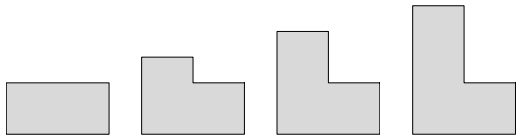

(a) 0.945 (b) 1.106 (c) 1.218 (d) 1.319

Figure 11: *I_s^c value for a rectangle and three L-shaped rooms.*

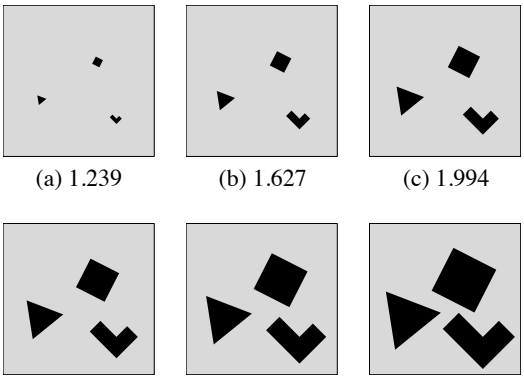

(a) 1.239 (b) 1.627 (c) 1.994

(d) 2.342 (e) 2.712 (f) 3.118

Figure 12: *I_s^c value for six scenes with three increasing size objects.*

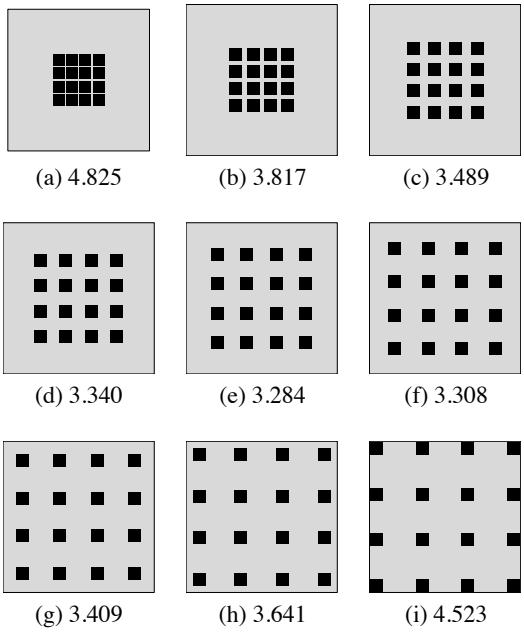

(a) 4.825 (b) 3.817 (c) 3.489

(d) 3.340 (e) 3.284 (f) 3.308

(g) 3.409 (h) 3.641 (i) 4.523

Figure 13: *I_s^c value for nine scenes which represent an expansion of 16 squares from the center of a square to its walls.*

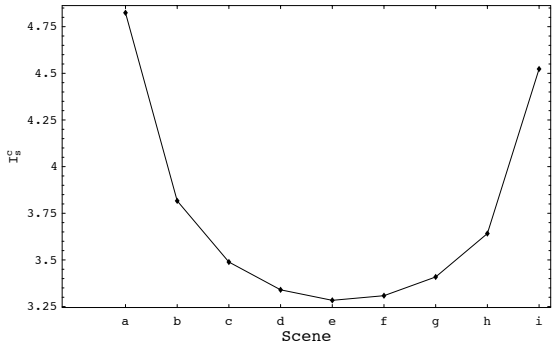

Figure 14: *Representation of I_s^c value corresponding to expansion of figure 13.*

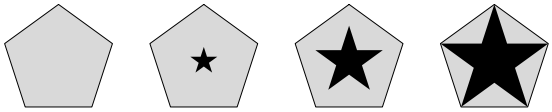

(a) 0.583 (c) 1.450 (f) 2.481 (i) 4.067

Figure 15: *I_s^c value for a pentagon and three scenes with a pentagonal star which grows until it almost touches the vertexs of the enclosure.*

The importance of the size of the objects is obvious in figure 12. We have seen that the introduction of objects increases complexity, but the interaction between the objects themselves and the enclosure depends clearly on their relative size: in general, the bigger the objects, the greater the complexity. In figure 13, the scene begins with 16 squares almost touching each other and ends with the 16 squares almost touching the edges of the enclosure. We can see (figure 14) that complexity is maximum in the first and last scenes and minimum in the middle scene.

After these sequences of scenes, we can confirm that the increase in corners or the creation of closer corners or spaces produces an increase in complexity.

4.2. Increase in complexity near singularities

In this section, we study the evolution of three groups of scenes. In the first case, a pentagonal star grows until it al-

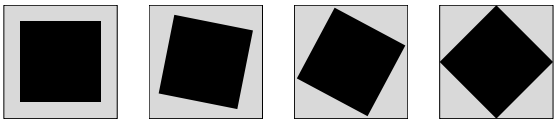

(a) 3.216 (c) 3.235 (f) 3.340 (i) 3.477

Figure 16: *I_s^c value for a scene with an interior square which rotates until its vertexes almost touches the enclosure.*

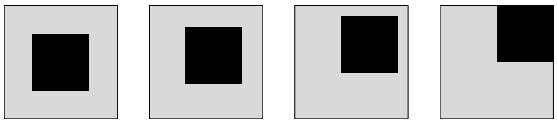

(a) 2.272 (c) 2.308 (f) 2.520 (i) 3.304

Figure 17: *I_s^c value for a scene with an interior square which advances until almost touching the walls of a corner.*

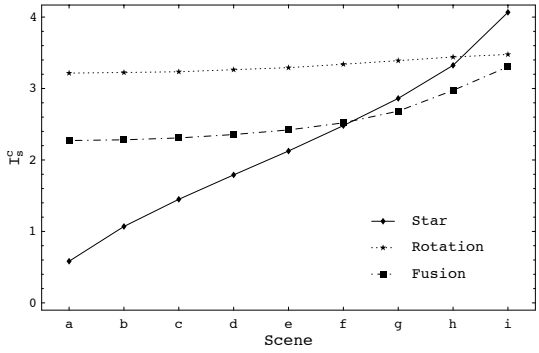

Figure 18: *Representation of I_s^c value corresponding to the scenes in figures 15, 16 and 17.*

most touches the vertexes of a pentagonal enclosure. In the second case, an interior square rotates in a square enclosure from a position with parallel sides to a position where the vertexes of the interior square almost touch the enclosure. In the third case, an interior square advances until almost touching the walls of a corner in a square enclosure.

In figure 15, a singularity is produced when the points of the star touch the vertexes of the pentagon. In this case, we obtain five independent scenes. Nearly the same happens with a rotating square (figure 16).

When the vertexes of the pentagon (figure 15) or the square (figure 16) almost touch the respective enclosure, it is easy to see that the mutual information is almost equal to the mutual information of a subscene plus the logarithm of the number N of equal subscenes (about to be) created:

$$\begin{aligned} I_s &\simeq N \sum_{i=1}^{n_s} \sum_{j=1}^{n_s} \frac{L_i F_{ij}}{L_T} \log \frac{F_{ij} L_T}{L_j} \\ &= \sum_{i=1}^{n_s} \sum_{j=1}^{n_s} \frac{L_i F_{ij}}{\frac{L_T}{N}} \log \frac{F_{ij} \frac{L_T}{N}}{L_j} + \log N \\ &= I_{subscene} + \log N \end{aligned} \tag{22}$$

where n_s is the number of patches of the subscene. The results are shown in table 4.

In figure 17, a singularity occurs when the internal square adheres to the right upper hand corner of the square, and thus recreates the L-shaped room as in figure 11(c). So, we

	square fusion	*pentagonal star*
$I^c_{subscene}$	1.474	1.750
number of subscenes (N)	4	5
$\log N$	2	2.322
$I^c_{subscene} + \log N$	3.474	4.072
I^c_s	3.477	4.067

Table 4: *Analysis of I_s^c value for figures 17(i) and 15(i).*

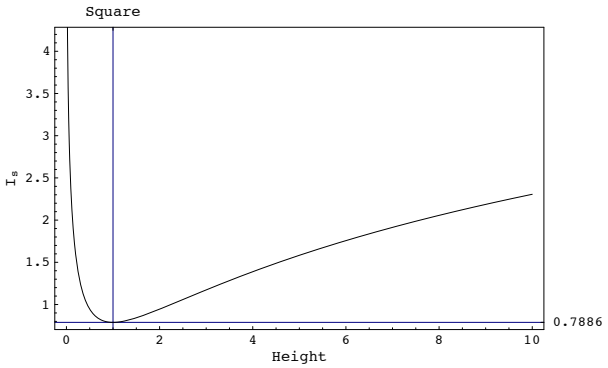

Figure 19: *Analysis of I_s^c value for a rectangle.*

can see that when we convert a square scene with a square object inside it to an empty L-shaped scene, this produces a collapse in complexity

$$I_s^c(figure\ 17(i)) = 3.304 \Rightarrow I_s^c(figure\ 11(c)) = 1.218$$

Figure 18 shows the evolution of the three sequences of scenes which we have just discussed. We can observe that the scene with the rotating square has the most stable complexity. In the star scene, as the size of the star increases so the correlation of the scene dramatically changes.

The strongest singularity is produced when the space between the edges disappears. Figure 19 shows that when the height of a rectangle tends to zero, complexity tends to infinity. The same happens with concentric circles, concentric squares, and so on. In conclusion, complexity grows near singularities.

4.3. Scene classification

From discussion in sections 4.1 and 4.2, we present a tentative scene classification:

- Low complexity: Simple empty scenes (without objects), like regular polygons, an isosceles right-angled triangle,

or scenes with few objects of low relative size, as in figure 12(a,b,c).

- Medium complexity: Scenes with few big objects, as in figure 12(d,e,f), scenes with more objects but with low relative size, as in figure 13, or scenes with edges not to close to each other, as in figures 16 and 17.
- High complexity: Scenes with a lot of objects, as in figure 4, or scenes with very narrow spaces, as in figure 8.
- Very high complexity: When all the edges of the scene are very close to each other, like very close concentric circles, a rectangle that is so long and narrow that it looks like a line, or a fractal scene whose walls form continuous almost closed cavities until to infinity.

5. Conclusions

In this paper we have defined the scene visibility complexity in flatland and analyzed its behaviour in relation to quantity, size and position of the objects within the scene, form of the enclosure and number of patches. We have also analyzed the growth of complexity when the scene is close to a singularity. Finally we have presented a preliminary scene classification.

6. Acknowledgements

Many thanks to J. Gelabertó. This project has been funded in part with grant numbers TIC 98-586-C03 and TIC-98-973-C03 of the Spanish Government.

References

1. BADII, R. AND POLITI, A. *Complexity. Hierarchical structures and scaling in physics*. Cambridge University Press, 1997.
2. BLAHUT, R.E. *Principles and practice of Information Theory*. Addison-Wesley, 1987.
3. CAZALS, F. AND SBERT, M. *Some Integral Geometry tools to estimate the complexity of 3D scenes*. INRIA Research Report 3204, July 1997.
4. COVER, T.M. AND THOMAS, J.A. *Elements of Information Theory*. Wiley, 1991.
5. CRUTCHFIELD, J.P. AND SCHALIZI, C.R. Thermodynamic depth of causal states: Objective complexity via minimal representations. In *Physical Review E* 59:275–283, 1999.
6. FEIXAS, M., ACEBO, E. AND SBERT, M. Entropy of scene visibility. In *Winter School on Computer Graphics and CAD Systems'99 (Plzen, Czech Republic)*, February 1999.
7. FEIXAS, M., ACEBO E., BEKAERT, P. AND SBERT, M. An information theory framework for the analysis of scene complexity. In *Computer Graphics Forum (Eurographics'99 Proceedings, Milan, Italy)*, 18(3):95–106, 1999.
8. FEIXAS, M., ACEBO E., BEKAERT, P. AND SBERT, M. Information theory tools for scene discretization. In *Rendering Techniques'99 (Proceedings of the 10th Eurographics Workshop on Rendering, Granada, Spain)*, Springer Computer Science, pp. 103–114, June 1999.
9. FELDMAN, D.P. AND CRUTCHFIELD, J.P. Statistical Measures of Complexity: Why?. In *Physics Letters A*, 238:244–252, 1998.
10. FELDMAN, D.P. AND CRUTCHFIELD, J.P. *Discovering Noncritical Organization: Statistical Mechanical, Information Theoretic, and Computational Views of Patterns in One-Dimensional Spin Systems*. Santa Fe Institute Working Paper (Santa Fe, USA), 98–04–026, 1998.
11. FELDMAN, D.P. *A brief introduction to: Information Theory, Excess Entropy and Computational Mechanics*. Department of Physics, University of California (Berkeley, USA), July 1997.
12. GORAL, C.M., TORRANCE, K.E., GREENBERG, D.P. AND BATTAILE, B. Modeling the interaction of light between diffuse surfaces. In *SIGGRAPH'84 Conference Proceedings (Minneapolis, USA)*, 18(3):213-222, July 1984.
13. HECKBERT, P.S. *Simulating global illumination using adaptive meshing*. Technical Report UCB/CSD 91/636, Computer Science Division (EECS), University of California (Berkeley, USA), June 1991.
14. LI, W. On the relationship between complexity and entropy for Markov chains and regular languages. In *Complex Systems*, 5(4):381-399, 1991.
15. MOTWANI, R. AND RAGHAVAN, P. *Randomized Algorithms*. Cambridge University Press, New York, 1995.
16. ORTI, R. *Radiosité Dynamique 2D et Complexe de Visibilité*. PhD. thesis, Université Joseph Fourier (Grenoble, France), July 1997.
17. RUBINSTEIN, R.Y. *Simulation and the Monte Carlo method*. John Wiley & Sons (New York, USA), 1981.
18. SBERT, M. An integral geometry based method for fast form factor computation. In *Computer Graphics Forum (Eurographics'93 Preoceedings)*, 12(3):C409–C420, September 1993.
19. SBERT, M. *The use of global random directions to compute radiosity. Global Monte Carlo methods*. PhD. thesis, Universitat Politècnica de Catalunya (Barcelona, Spain), March 1997.
20. SBERT, M., PUEYO, X., NEUMANN, L. AND PURGATHOFER, W. Global multipath Monte Carlo algorithms for radiosity. In *The Visual Computer*, 12(2):47–61, 1996.